Chapter 3

$N^{O}E$ Experimental Apparatus

3.1 Detector

3.1.1 Conceptual Design

The proton luminosity of present accelerator, Tab. 2.2, generates a neutrino flux that, according to $1/L^2$ behavior, is relatively low in a far detector. Such a long baseline neutrino beam can produce about 1 - 2 thousand detected events per year, per kiloton in a detector placed about 700 km far from the source. Therefore, due to the small cross section of neutrinos and to relative low neutrino flux, an optimal detector must have the largest possible target mass compatible with the underground location. In general several kilotons are needed to reach a sensitivity in $\sin^2 2\theta$ of the order of $\sim 10^{-2}$.

It is worth noting that, assuming a reasonable cost, the level of granularity of the detector strongly depends on the mass. This leads to a compromise between total mass and granularity. In fact the number of events increases with the total mass, but the quality of measurements is improved with higher granularity. So the choice of the most suitable mass depends on the measurement criteria adopted to reach the experimental goals. On one hand, some processes investigated to study ν_μ oscillations are relatively insensitive to granularity and the accuracy in their measurement is only limited by statistics; on the other hand, other processes require a higher granularity even at the expense of statistics.

In the following, main possible approaches to get oscillation signal are reported:

1. Measurement of the ratio of hadronic shower events without muon track (apparent NC events) to those with a muon track (apparent ν_μ CC

events). This measurement not only provides a clear signature of muon neutrino disappearance (muon deficit), but it is also sensitive to ν_τ appearance due to hadronic decay of τ's. In fact the ratio NC/CC=$\frac{no\mu}{\mu}$ should change if $\nu_\mu \rightarrow \nu_e$ or $\nu_\mu \rightarrow \nu_\tau$. This statistical measurement requires a large mass and consequently a poor granularity.

2. Comparison of the interaction rates (ν_μ CC events and apparent ratio NC/CC events) in a near and far detector. A detector located close to the accelerator allows a comparison between neutrino interactions in the two detectors at different distances from the neutrino source. Also this measurement needs a large number of events and conseguently a very massive far detector. In addition, a similar near detector is required to minimize beam and detector systematics.

3. Search for τ or electron appearence reconstructing the events. The detector devoted mainly to this measurement must have very high granularity rather than a large mass. A beam monitor, identifying ν_e beam background, could be useful for this kind of analysis.

N^OE experiment privileges the last method. At present, the general design choice is to have a moderate but fully active mass and high granularity, allowing a fine event reconstruction. It is noteworthy that this feature is remarkable also for low energy atmospheric neutrino events, to improve electron and muon recognition.

The analysis of events will be described in detail in Chapters 6 and 7. First of all it requires the identification of muons and a good measurement of their energy and angle of production respect to the beam direction. Streamer Tubes or better Resistive Plate Counters are mainly addressed to this last item. In addition electromagnetic and hadronic showers have to be identified and characterized in direction and energy.

Good total energy measurement and fine longitudinal and transverse energy sampling is mandatory in order to evaluate discriminating kinematical parameters like coplanarity, missing energy and transverse energy of the events. Specifically these parameters are required in order to identify presence and decay of τ leptons generated by ν_τ CC. To perform accurate measurements of shower characteristics a homogenous fine grain calorimeter based on scintillating fiber technology is chosen. At present the cost of readout electronics limits the intrinsic granularity of the detector; the best readout choice for reconstructing signal and background events is under investigation.

An apparatus completely equipped with fast detectors would allow to lower the energy threshold of the detected events: the short time coincidence allows to reduce the number of elements and hence the amount of material required to have a trigger. The combination of fast scintillating fibers and resistive plate counters (fast tracking) could be the best solution, mainly for atmospheric neutrinos whose event rate depends on the energy threshold. In addition a fast detector allows to distinguish π, K and μ decays and the direction of the particles as well.

It is noteworthy that this experiment design conceived with such a type of detectors makes very easy the implementation of a smaller beam monitor.

In conclusion the philosophy of this design is to have oscillation sensitivity in two separate ways: by looking for event reconstruction of τ decay or for an electron excess respectively for $\nu_\mu \rightarrow \nu_\tau$, $\nu_\mu \rightarrow \nu_e$ and by measuring a deficit of muons in apparent NC/CC. The first method represents the priority of this proposal.

3.1.2 General Layout

The size and shape of the detector is decided on the need to get as large fiducial mass as possible for neutrino interaction and to provide a good particle containment as well. The necessity to have a massive target leads to a diffuse and homogeneous apparatus in which all parts work not only as a total active target but also as a complete detector (tracker, calorimeter, muon detector, etc). Fig. 3.1 shows an overview of full detector. To maximize a fiducial volume it has been calculated the optimum dimensions of the calorimeter for a chosen mass of 4 ktons. It is distributed in 4 blocks, 1 kton each. In addition, to recover the muons when the interaction occurs at the edges of the apparatus, a muon detector and a muon frame all around the fiducial volume have been inserted. The full length of the detector is 41 m with a total mass of 6 ktons.

The necessity of having a muon detector is explained taking into account that the containment energy for each block is about 8 GeV. The detector is modular and easily extendible.

3.1.3 The Calorimeter

The calorimeter technique of embedding scintillating fibers into an absorber has been developed in the past years and recently used in CHORUS[1] and KLOE [2] experiments. The calorimeter described in the following is a fur-

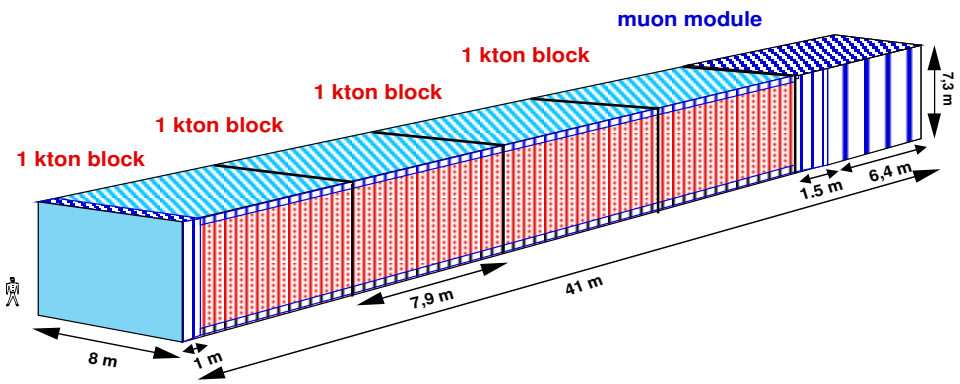

Figure 3.1: Overview of the $N^{O}E$: Neutrino Oscillation Experiment

$\%Fe$ (Weight)	BCE W tons	Xo cm	λ cm	$<\rho>$ g/cm^3	$<Z>$	E_c MeV
70	0.5	5.6	44.5	3.0	15.2	49.

Table 3.1: Main features of the iron ore (hematite).

ther evolution of this technique particularly addressed to massive detector. The calorimeter is located in the inner part of the detector. Each 1 kton calorimetric block, presented in Fig. 3.2, is $(7.9 \times 7.3 \times 8)$ m^3 large, composed by **Basic Modules (BM)** $0.13 \times 0.52 \times 8$ m^3, 2 tons each, logically divided in four **Basic Calorimetric Elements (BCE)** , $0.13 \times 0.13 \times 8$ m^3.

The basic calorimetric element can be realized as follows: the element is made by an ~ 8 meters long bar of an iron ore as radiator with scintillating fibers as active component, suitably distributed in the bar and parallel to the axis. Iron ore has two advantages:

- the first is the radiopurity. Fig.3.3 shows radioactivity spectrum of an iron ore sample, after the subtraction of the environmental radioactivity. It can be inferred from this figure that the iron ore is like a sort of screen against natural radioactivity, and it does not introduce further contributions to the background. The very low level of iron ore background leads to a low single counting rate of the BCE element, particularly suitable to implement soft triggers.

- the second is that the iron ore is practically cost free.

The cross section of the element is a square 13 cm side. The weight is about 0.5 tons and the thickness ~ 2 radiation lengths. Anyway it has to be noted that these radiation lengths are completely active.

The number of fibers and their positions in the BCE element have been optimized by means of a Monte Carlo procedure. In order to guarantee the detector isotropy, the fibers are randomly located inside the bar (Fig. 3.4).

Fig. 3.5 shows the total thickness of the active part (scintillator) crossed by a minimum ionizing particle (muon) going through the BCE element. The geometrical efficiency for the single BCE is 98%.

In each element there are 330 fibers, 2 mm in diameter, viewed at each end, in the most conservative hypothesis, by one 2" photomultiplier. The very low cost HAMAMATSU R5686 PMT fits well fibers features.

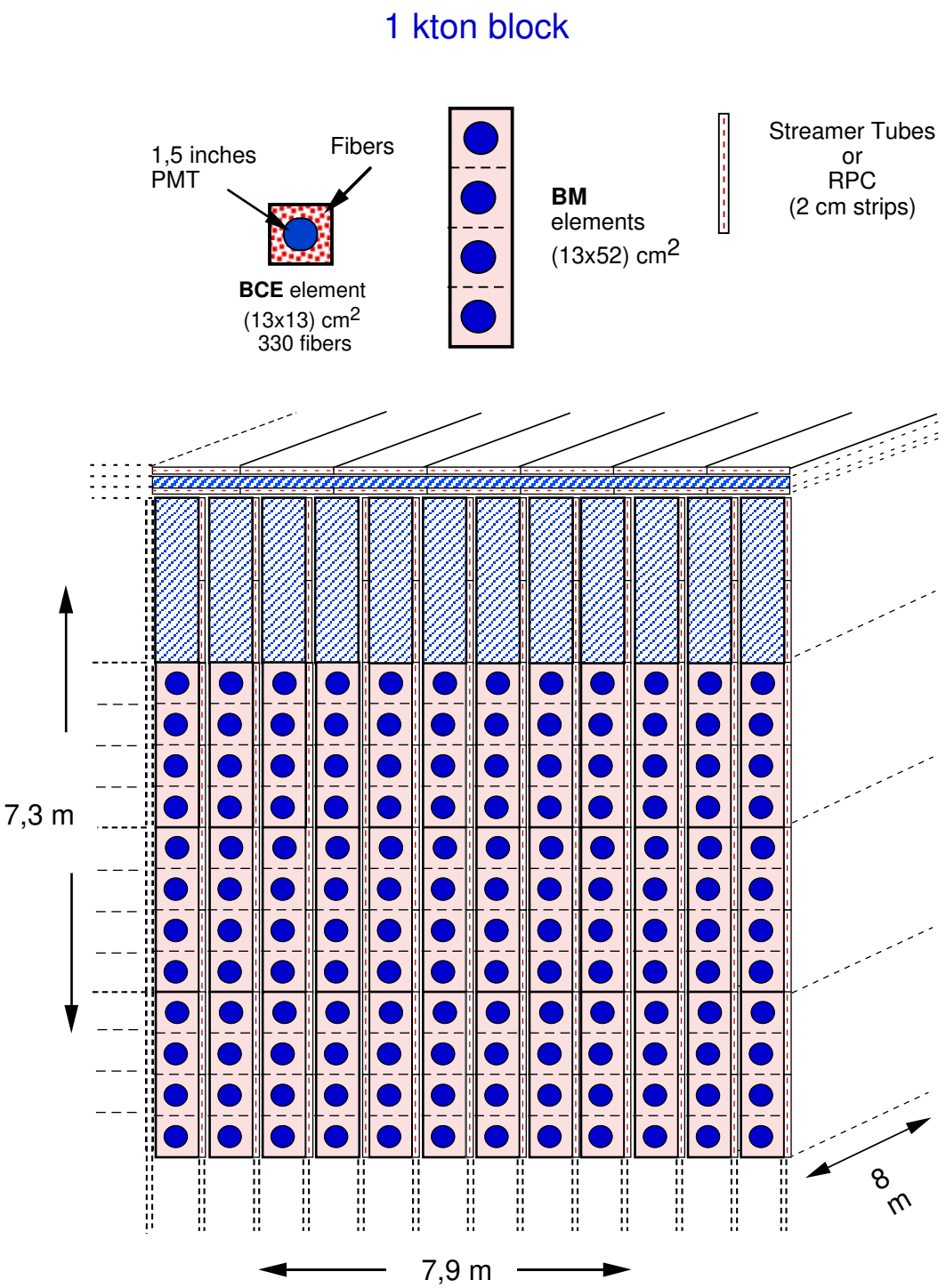

Figure 3.2: Details of $NO\nu E$ calorimeter

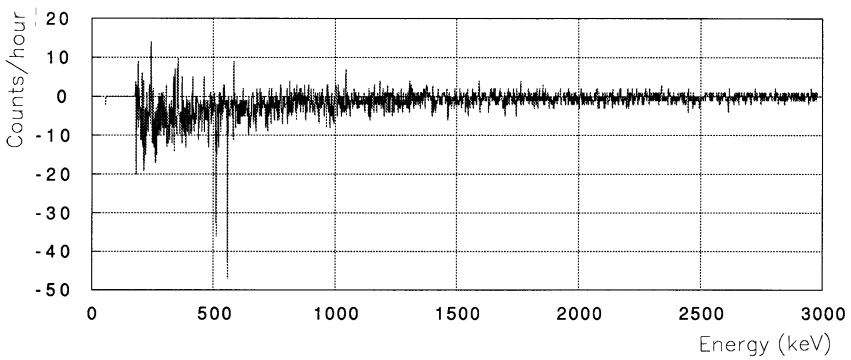

Figure 3.3: The radioactivity spectrum of an iron ore sample, after the subtraction of the environmental radioactivity.

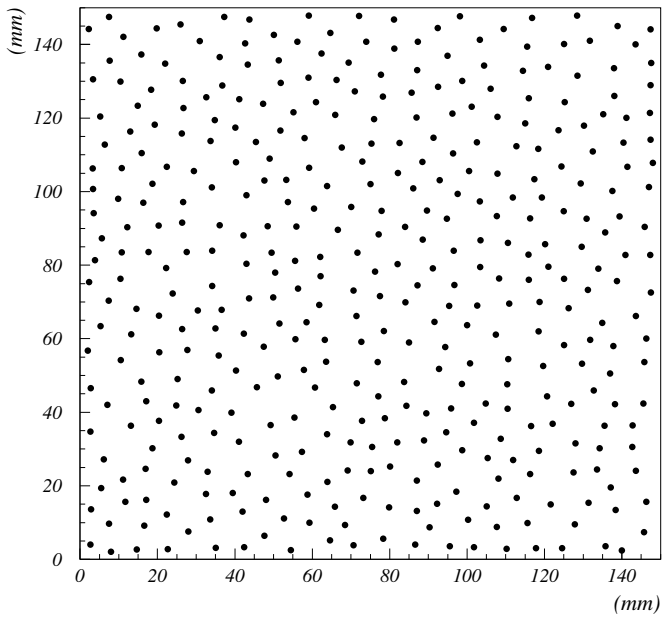

Figure 3.4: Cross section of basic calorimetric element (BCE).

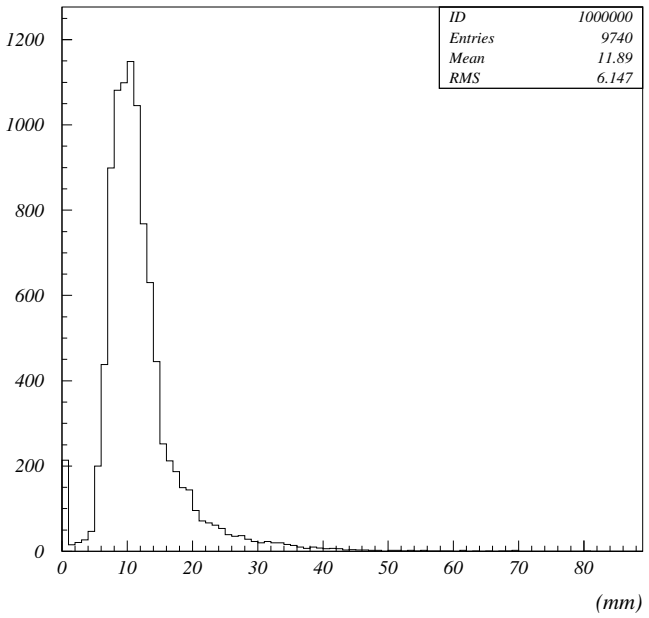

Figure 3.5: Total thickness of active part (scintillator) crossed when a minimum ionizing particle (muon) goes through the BCE element.

The fiber attenuation length now achievable ($5 \div 6$ m) allows to obtain a 8 m bar length. The fibers are protected by a low cost envelope and their positions are determined by masks set 1 m apart along the 8 m bar.

In the following the main features of this element are summarized:

- 13 cm side square (~ 2 active radiation lengths)
- 330 scintillating fibers, 2 mm in diameter, as active component
- Fiber attenuation length ($5 \div 6$) m
- Iron ore as radiator

At present this design seems to be quite satisfactory. However the final choice of the bar parameters will be the best compromise among granularity, fiber numbers, weight, radiation length, light yield and cost.

A possible option exists for the BCE element. Plastic tubes, teflon coated, filled with liquid scintillator could be used as active part. Taking into account the different refractive index and the good light transmission of the scintillator, this detector could be a good optical wave guide may be more efficient and at lower cost with respect to the fibers.

Detector development efforts towards both the solutions of the active part is planned to determine the best final choice. Four Basic Calorimetric Elements together form a module of 2 tons, 1320 scintillating fibers. This modularity has to be repeated in order to reach a 1 kton block volume. The whole calorimeter has about 8000 BCE in 185 layers. Many solutions for the construction of the calorimetric bars are under study.

3.2 Tracking System.

The tracking detector, interleaved between vertical calorimetric modules, can be realized by means of limited streamer tubes (LST) or resistive plate counters (RPC), both with a thickness of $\sim$ 2 cm.

The LST [3] system has a modular structure, consisting of a basic cell ($2cm \times 2cm \times 8m$) with an anode wire on its axis. A certain number (tipically 8) of basic cells are contained in a chamber. Pick-up strips (2 cm wide) can be mounted perpendicularly to wires in order to get readout in the other view. The typical gas mixture for LST contains Ar and one or more hydrocarbons as quencher (typically isobutane). Anyway for safety reasons and taking into account that the tubes are slaves (the fast trigger is given by the calorimeter elements), non flammable mixtures can be used. Recent studies have shown that satisfactory operation can be obtained with a mixture containing few parts of isobutane ($< 10\%$) and CO_2 percentage greater than 80%. Also attempts with Ar and CO_2 mixtures could be done. Anyway it is necessary to remind that safety problems connected with streamer tube gas have been already solved and large underground detectors are operating since many years [7]. The need of streamer tubes for the whole apparatus is 79,000 wires that means 13,000 m^2.

The RPC is a DC operated gas device working in limited streamer mode [4, 6, 5]. Fig. 3.6 shows a transverse view of such a device. The required high field (40 kV/cm) is generated by a thin layer of graphite which coats the outside surfaces of two parallel plates of 2 mm thick bakelite. When an ionizing particle crosses the gas gap (2 mm) between the bakelite plates the streamer is quenched by the prompt switching off of the local field around the discharge point due to the high resistivity of the electrodes and by the action of the gas. Spacers between bakelite plates give rise to some dead zone in the chamber. However two parallel chambers with staggered spacers can be used (double gap RPC).

The generated pulse is read out by means of external pick-up strips or

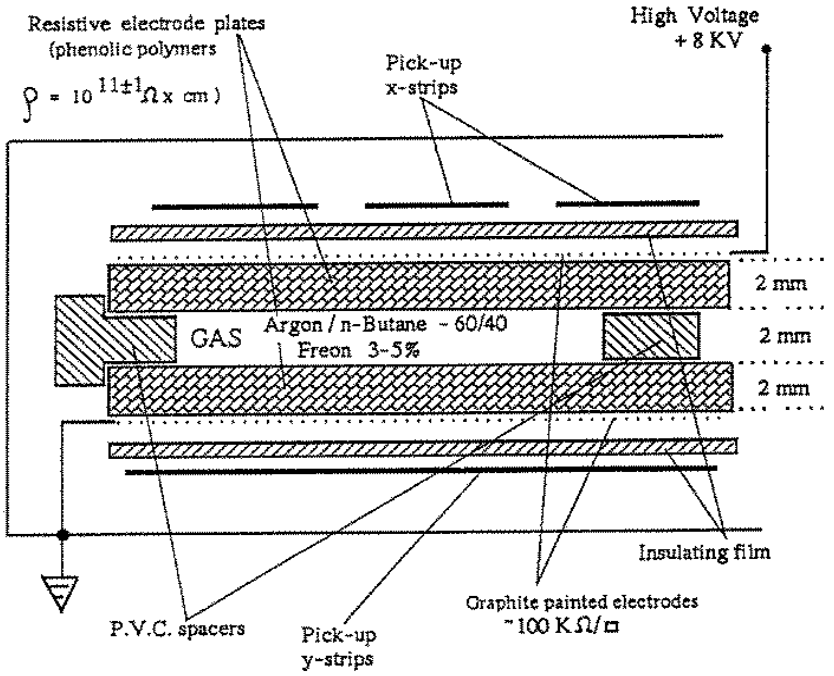

Figure 3.6: RPC stratigraphy.

pads. In $N^O E$ case, in order to obtain an XY view, two layers of perpendicular strips can be mounted on both sides of the chamber.

The main peculiarity of the RPC is the reduced size of the gas gap which allows a very intense and uniform electric field. Under these conditions, the formation of the streamer occurs in a very short time and with minimal fluctuations. The time resolution results to be of the order of 1 ns or less and the time delay between the passage of a particle and the signal formation is $\sim$ 10 ns.

The typical gas mixture used is 55% Ar, 41% normal butane (for the absorption of the ultraviolet photons), 4% freon 13B1 (for the capture of peripheral electrons around the streamer). Other mixtures without butane and freon have been tested, in order to avoid safety and environmental problems.

The RPC are currently produced in standard dimensions ($1 \times 2m^2$ or $1.5 \times$

$2.5m^2$). Assembling togheter 3 RPC of slightly non-standard dimensions, it is possible to get a module compatible with the transverse NOE dimension (7 m).

RPC with plates in glass instead of bakelite and of dimensions suitable to fit the length of a BCE module are also under study. This last solution has the advantage to reduce the dead zones due to spacers and frames, because glass provide a more rigid structure.

The absence of wires makes the RPC easier to assemble and less susceptible to failures. Moreover the good timing properties improve the NOE fast timing response (see Sec. 3.1.1).

Fig. 3.7 shows knee and efficiency of the plateau for a single gap RPC as functions of argon/butane ratio with 5% freon fraction. The limiting efficiency is due to the dead zones around the spacers [8]. Fig. 3.8 shows the efficiency and time resolution as functions of high voltage for a double gap RPC with a safe gas mixture [9].

3.2.1 The Muon Detector

A module made of tracking detectors and iron ore is placed at the end of the whole apparatus (Fig. 3.1). The purpose of this 1 kton module is to recover muons produced in charged current interaction of ν_μ beam occurring in the final calorimetric block.

The absorber consists of 30 layers built with BM modules filled with iron ore and without active part inside. The tracking layers are 21 interleaved in between the absorber.

The first 1.5 meters of the module have with the same modularity of the calorimetric block, in order to get more information about hadronic showers accompanying the muons in interactions occurring at the end of the last calorimetric block. A length of about 2 m matches the average depth of hadronic shower development (Fig.5.5). In the second part, the active planes are one for each two absorber layers.

In addition the frontal, the upper and the bottom part of the whole detector are covered by a 1 kton frame, in which tracking detectors and absorber are interleaved. As for the muon detector the purpose of this part is to increase the fiducial volume recovering muons generated in the calorimeter boundary.

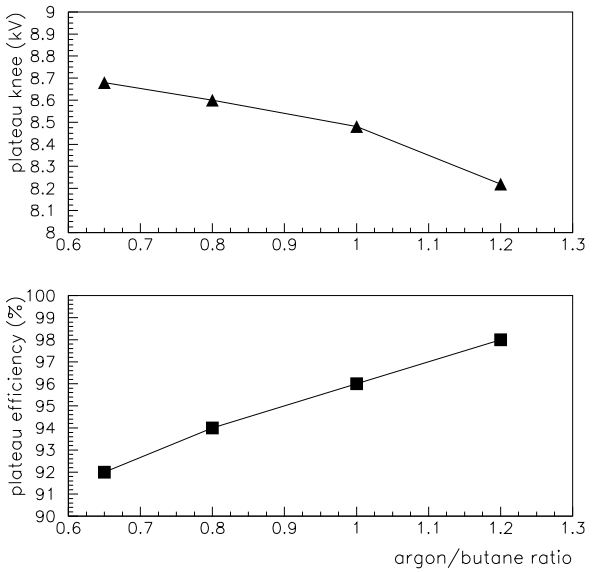

Figure 3.7: Efficiency and plateau knee vs the ratio butane/argon for a single gap RPC.

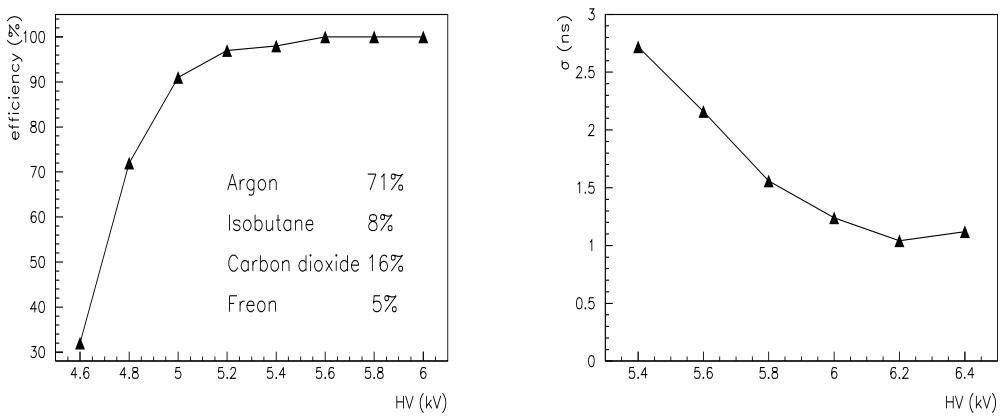

Figure 3.8: Efficiency plateau and time resolution for a double gap RPC.

3.3 Trigger and Readout

3.3.1 Trigger

The scintillator, inside the calorimeter, is a very fast detector and makes possible short time coincidences. RPC trackers, as well, gives fast timing response. Hence 100, 200 ns should be the resolution time of the event. Combining both this feature and low rate of background due to the excellent iron ore radiopurity, it will be possible to implement soft trigger to lower the energy threshold ($E_{thr} \sim 300 \div 400$ MeV). It represents an important feature of the experiment particularly for atmospheric neutrino studies. Being RPC trackers interleaved between the calorimetric walls, the requirement of one BCE crossed by a particle, implies a three-fold coincidence (2 RPC + 1 BCE), and in general the request of n BCE crossed implies (2n+1)-fold coincidence.

Since the number of radiation length in a single BCE is about 2 (see Table 3.1.3), the previous relation includes the requirement that a particle crosses about 2n radiation length of absorber material before the trigger is fired.

In addition to the trigger logic based on geometrical configuration, a more homogenous one could be implemented requiring a minimum total released energy. The energy threshold will be defined as a consequence of the background energy spectrum.

3.3.2 Readout electronics

As described above, $N^O E$ apparatus has two type of active detectors: tracking detectors (Streamer tubes or RPCs) and calorimetric detector (Scintillating fibers viewed by 1.5 inches PMT's). The total number of channels (wire-strips) of the tracking system is about 176,000, while the 4 ktons calorimeter has about 16,000 channels to be read out. Obviously the two systems need very different electronic front-end readout while only minor differences are supposed between front-end electronics for RPCs and Streamer tubes. (Discriminators, fast OR etc.)

3.3.3 Tracking readout electronics

The front end electronics for the tracking system, as usual in big apparata, will be distributed along the detector in order to minimize distances travelled by analog signals. The readout board will perform the standard front-end electronics functions (amplification if necessary, discrimination and shaping of the digital signals) and moreover, using custom chips, a first level zero

suppression. A number of cards (32 channels each) will be connected by a parallel bus and controlled by a VME-based controller. This controller provides to the cards the threshold value for discriminators, the width of the digital signals and enables test cycles to check the performances of each board channel by channel. Moreover it performs residual zero suppression, labels data with trigger number and codes data in order to recognize where they come from. To minimize the number of controllers it is important to connect the maximum number of readout cards to the same controllers increasing the total length of the connecting bus. To overcome possible problems due to the bus length it is planned to use a point to point architectures like Token ring. The current plan is that the VME-based controller will handle two contiguous planes (about 1,600 channels). In this case the total number of VME boards to read out the whole tracking system will be about 110 which need 7 VME crates.

In the current approach the N^OE DAQ system is a trigger-driven environment, where all the acquisition boards and the readout controllers share the same trigger signal. When a trigger pulse is issued by the main trigger system, each DAQ board increments an on board trigger counter. The slave boards (VME boards) label the acquired data with the actual trigger number and push the data frame in a buffer. The controllers read out the DAQ boards on a trigger number basis. In this way the event-building phase starts at early stage of the data acquisition.

3.3.4 Calorimeter electronics

For each channel of the calorimeter it is necessary to store the charge, the arrival time as well as the width of the signals. Moreover to observe delayed events like muon decay, for each trigger, signals in a temporal window of several microseconds must be recorded. In a standard approach a multihit ADC and a multihit TDC (both edges sensitive) for each channel are needed. The Fig. 3.9, obtained by a Monte Carlo simulations, shows that in order to measure high charges, due to energy released by electromagnetic and hadronic showers, good linearity over a factor 50 in dynamics is needed. Therefore resolution and dynamic range foreseen for the ADC are respectively 0.25 pC and 50 while for TDC are respectively 1 ns and 15 μs. The plan is to develop an electronics board able to include all these functions using the same approach used for instance by the MACRO collaboration [10].

The Fig. 3.10 shows a very preliminary block diagram of one channel. The time over threshold discriminator provides to the TDC the two edges to

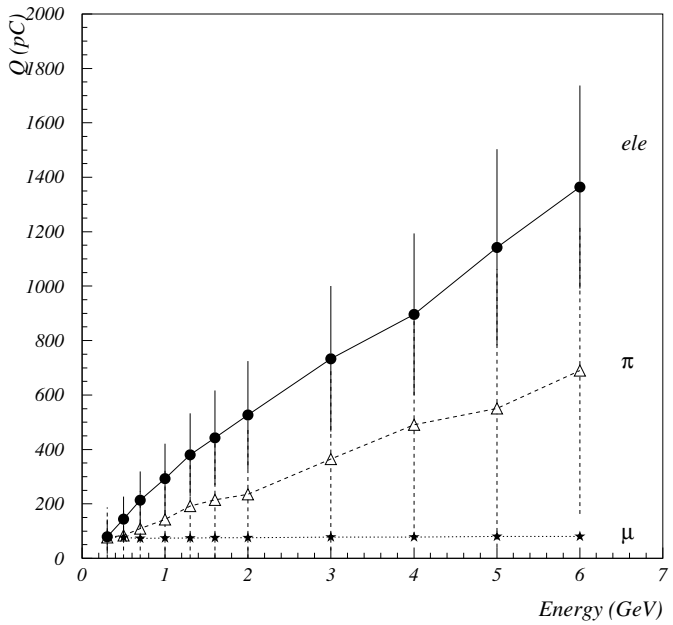

Figure 3.9: Simulated charge dynamic range for different particles as a function of the incident energy.

measure arrival time and width of the signals while the charge is obtained from the 11 bit flash ADC after integration. All the informations are registered in a FIFO memory. Different solutions for each block are now under study. Using in massive way custom chips it is planned to contain at least 32 channels in a single VME-based board (6U or 9U). In this hypothesis the total number of VME boards for the calorimeter read out is about 500 for a total of about 30 VME crates.

3.3.5 DAQ

The $N^{O}E$ data acquisition system will be implemented in VME standard. Nowadays, VME is a robust reliable protocol widely used in physics applications as well as in industrial environments. Many vendors offer low to high end CPUs and peripheral boards with plenty of real time operating systems to choose from. This fact makes the VME the ideal platform to develop an high performance DAQ system.

Complex DAQ architectures need specific channels for debugging, performance monitoring as well as system booting. On the other hand, the

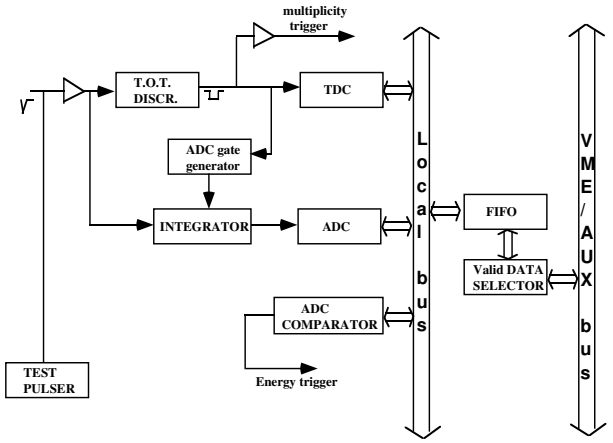

Figure 3.10: Block diagram for calorimeter front-end electronics.

$N^{O}E$ DAQ deals with very severe requirements in terms of data transfer rate, event-building protocols and data integrity checking. A suitable architecture which allows I/O intensive applications, can be based on synergies between VME and an auxiliary custom bus, as shown in Fig. 3.11. Such a perspective has been evaluated by the KLOE collaboration [11]. The $N^{O}E$ DAQ system could benefit the same approach, using custom buses for data acquisition and event building. In the $N^{O}E$ detector only a few percentage of channels are fired in a typical event. The DAQ system hence needs sparse data scan capability to read out, for each event, only the boards with valid data. To improve the transfer rate, the I/O operations should proceed in a block fashion. The VME protocol is not optimized for both such applications. No sparse data scan is allowed at crate level and block transfer performances suffer from the deterministic size of the DMA cycles and the software penalties. The AUX bus protocol developed for the KLOE experiment offers high speed sparse data scan cycles to locate board with valid data. It also handles random length block transfer without any software overhead, with a sustained data rate in excess of 10 MHz. In this environment, the VME is left fully available to run monitoring programs and to spy the online data flow.

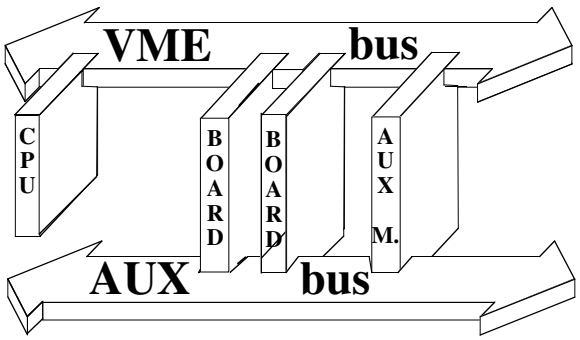

Figure 3.11: Schematic diagram of $N^{O}E$ DAQ.

3.4 High Granularity Readout

3.4.1 General Considerations

A simple way to read a BCE element is by grouping all the fibers at each side on 2 inches PMT. This experiment wants to address the fibers readout towards a finer configuration giving more event topology informations.

Dividing the end section of BCE in a grid in which every group of fibers is coupled to a multianode device, a good pattern recognition of the event can be reached (Fig. 5.12). The grid digital hits will be sent to a shift register chain, whereas energy loss and crossing time are achieved OR-ing the grid signals. To date a simple and compact multianode PMT 4×4 (HAMAMATSU H6568) is available for this purpose. In order to reduce the cost of the grid readout, the possibility to instrument only the fiducial volume of the calorimeter can be considered (full grid readout in the fiducial volume). Otherwise the grid readout can be implemented only on one side of BCE bar, whereas on the other one the fibers are grouped in a classic way with one PMT (half grid read out in the total volume), as shown in (Fig. 3.12). The last method will be interesting if the attenuation length will increase significantly in the future. The simulation, still in progress, will

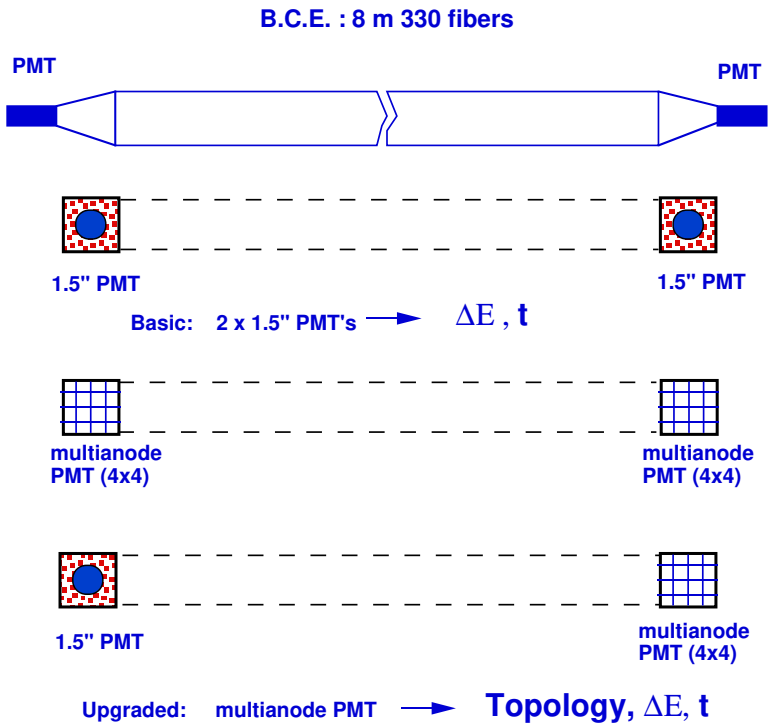

Figure 3.12: The electronic readout for the basic calorimetric element (BCE)

suggest the more suitable grid read out to improve either electromagnetic and hadronic shower discrimination, or their direction measurements. This point will be further discussed in the Section 5.3.

It is worth remarking that the ability of knowing as correctly as possible the geometrical parameters of the event (coplanarity, direction of the shower axis, etc.) allows to increase the resolution in the missing P_t when the τ lepton in ν_τ CC is produced. Hence, three independent measurements can be carried out by $N^O E$ experiment for this purpose: center of gravity respectively of transverse energy distribution, tracking hits and grid readout hits. Due to the large mass of the future experiments and to the request of having finer reconstruction of events, a big number of channels will be required. Therefore the possibility of having a new high technology devices at low cost would be very appealing.

3.4.2 HPD readout option

Recently many effort have been devoted to develop a new fast light device, hybrid photodiode (HPD), with a very simple structure, high linearity and great reliability [12].

HPD tube is made of an ordinary photocathode mounted in front of a planar semiconductor diode. In between there is a vacuum gap held at a voltage of a few kVolts. This kind of detector shows good performances in linearity, stability and speed. Since the photocathode is imaged on silicon chip, by subdividing the silicon diode in pixels, HPD can become a position sensitive device very useful for $N^{O}E$ purpose in order to reconstruct the event topology.

3.4.3 CCD Readout Option

The maximum of the topological resolution in the readout of the BCE can be reached using an Image Intensifier (I.I.) followed by a CCD. Such device was used in UA2 [13] for particle tracking and in CHORUS [1] for calorimetry and it has been proposed for LHC [14]. It has been measured in preliminary tests (see Chap. 4) that for a m.i.p. crossing a single BCE, on average, 7 fibres are fired, everyone emitting 5 p.e. In principle these numbers are enough to allow the reconstruction of the event with high efficiency.

Both ends of the BCE must be instrumented with I.I. and CCD to catch the maximum number of photons generated inside the fibers.

The choice of RPC's as tracking detector for the $N^{O}E$ experiment allows to exploit the good time resolution of this type of detector to exhaust all needs for triggering and timing. In this way the lack of a fast signal from the BCE's, deriving from the use of I.I., does not downgrade the timing capability of the experiment giving on the other hand the highest spatial resolution.

The tentative scheme proposed for the BCE readout is shown in figure 3.4.3. Here an old type of I.I. is shown with the intent to emphasise only the principle of using Image Intensifiers. The field of the Image Intensifier is rapidly changing and more effective and economic solutions can be available on the market in the next future.

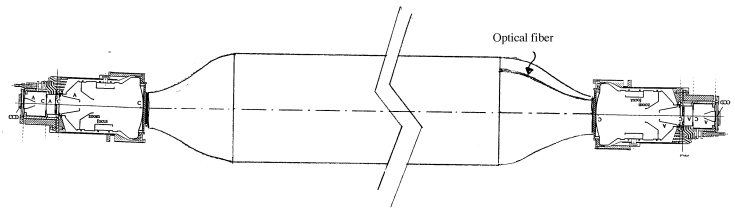

Figure 3.13: The scheme of BCE readout using image intensifiers and CCD.

Bibliography

[1] Chorus Coll., CERN/PPE/93-131 (1993)

[2] KLOE Coll., LNF 92/019

[3] E. Iarocci, Nucl. Instr. and Meth. 217 (1983) 30

[4] R.Santonico et al., Nucl. Instr. and Meth. 187 (1981) 377

[5] M.Ambrosio et al., Nucl. Instr. and Meth. A344 (1994) 350

[6] F. Grancagnolo, Proc. of the "4th topical Seminar on Experimental Apparatus for high Energy Particle Physics and Astrophysics", San Miniato, Italy, 1990

[7] S. Ahlen et al., Nucl. Instr. and Meth. A324 (1993) 337

[8] E. Gorini, INFN/AE-90/18 presented at the Second Intern. Conf. on Advanced Technology and Particle Physics, Como, Italy, 1990

[9] V. Arena et al., Nucl. Instr. and Meth. A360 (1995) 87

[10] M. Ambrosio et al.,Nucl. Instr. and Meth. A321 (1992) 609

[11] Aloisio et al., Proceedings of Conference Computing in High Energy Physics (1994) 430

[12] R. DeSalvo et al., Nucl. Instr. and Meth. A315 (1992) 375

[13] J. Alitti NIM A273(1988)135; R.E. Ansorge, NIM 265 (1988) 33

[14] CMS Coll., Letter of Intent, CERN/LHCC 92-3 (1992); ATLAS Coll., Letter of Intent, CERN/LHCC 92-4 (1992).